Neuro-Oncology

19(1), 31–42, 2017 | doi:10.1093/neuonc/now118 | Advance Access date 14 July 2016

Morphological and molecular features of astroblastoma, including *BRAF*^{V600E} mutations, suggest an ontological relationship to other cortical-based gliomas of children and young adults

Norman L. Lehman, Eyas M. Hattab, Bret C. Mobley, Aisulu Usubalieva, Matthew J. Schniederjan, Roger E. McLendon, Werner Paulus, Elisabeth J. Rushing, Maria-Magdalena Georgescu, Marta Couce, Mohanpal S. Dulai, Mark L. Cohen, Christopher R. Pierson, Jack M. Raisanen, Sarah E. Martin, Trang D. Lehman, Eric S. Lipp, Jose M. Bonnin, Mousa A. Al-Abbadi, Kara Kenworthy, Kevin Zhao, Nehad Mohamed, Guojuan Zhang, and Weiqiang Zhao

Department of Pathology, The Ohio State University, Columbus, Ohio (N.L.L., A.U., C.R.P., K.K., K.Z., N.M., G.Z., W.Z.); Department of Pathology and Laboratory Medicine, Indiana University, Indianapolis, Indiana (E.M.H., J.M.B.); Department of Pathology, Vanderbilt University, Nashville, Tennessee (B.C.M.); Department of Pathology and Laboratory Medicine, Emory University, Atlanta, Georgia (M.J.S.); Department of Pathology, Duke University, Durham, North Carolina (R.E.M., E.S.L.); Institute of Neuropathology, University Hospital Münster, Germany (W.P.); Institute for Neuropathology, University Hospital of Zurich, Switzerland (E.J.R.); Department of Pathology, The University of Texas Southwestern, Dallas, Texas (M.-M.G., J.M.R.); Department of Pathology, Case Western Reserve University, Cleveland, Ohio (M.C., M.L.C.); Department of Anatomic Pathology, Beaumont Hospital, Royal Oak, Michigan (M.S.D.); Department of Pathology and Laboratory Medicine, Nationwide Children's Hospital, Columbus, Ohio (C.R.P.); Department of Pathology, University of Illinois, Peoria, Illinois (S.E.M.); Department of Pathology, Sheikh Khalifa Medical City, Abu Dhabi, UAE (M.A.A.-A.); Department of Family and Community Medicine, Contra Costa Regional Medical Center, Martinez, California (T.D.L.)

Corresponding Author: Norman L. Lehman, MD, PhD, Division of Neuropathology, Department of Pathology, The Ohio State University Wexner Medical Center, Graves Hall, Room 4166, 333 West 10th Avenue, Columbus OH 43210 (nllehman@yahoo.com).

Abstract

Background. Astroblastomas (ABs) are rare glial tumors showing overlapping features with astrocytomas, ependymomas, and sometimes other glial neoplasms, and may be challenging to diagnose.

Methods. We examined clinical, histopathological, and molecular features in 28 archival formalin-fixed, paraffin-embedded AB cases and performed survival analyses using Cox proportional hazards and Kaplan–Meier methods.

Results. Unlike ependymomas and angiocentric gliomas, ABs demonstrate abundant distinctive astroblastic pseudorosettes and are usually Olig2 immunopositive. They also frequently exhibit rhabdoid cells, multinucleated cells, and eosinophilic granular material. They retain immunoreactivity to alpha thalassemia/mental retardation syndrome X-linked, are immunonegative to isocitrate dehydrogenase-1 R132H mutation, and only occasionally show *MGMT* promoter hypermethylation differentiating them from many diffuse gliomas. Like pleomorphic xanthoastrocytoma, ganglioglioma, supratentorial pilocytic astrocytoma, and other predominantly cortical-based glial tumors, ABs often harbor the *BRAF*^{V600E} mutation, present in 38% of cases tested (n = 21), further distinguishing those tumors from ependymomas and angiocentric gliomas. Factors correlating with longer patient survival included age less than 30 years, female gender, absent *BRAF*^{V600E}, and mitotic index less than 5 mitoses/10 high-power fields; however, only the latter was significant by Cox and Kaplan–Meier analyses (n = 24; P = .024 and .012, respectively). This mitotic cutoff is therefore currently the best criterion to stratify tumors into low-grade ABs and higher-grade anaplastic ABs.

Conclusions. In addition to their own characteristic histological features, ABs share some molecular and histological findings with other, possibly ontologically related, cortical-based gliomas of mostly children and young adults. Importantly, the presence of *BRAF*^{V600E} mutations in a subset of ABs suggests potential clinical utility of targeted anti-BRAF therapy.

Key words

astroblastoma | *BRAF*^{V600E} mutation | IDH1^{R132H} mutant protein expression | *MGMT* promoter hypermethylation | Olig2 protein expression

Astroblastomas (ABs) are rare glial tumors first described in the 1920s.[1,2] They most frequently involve the cerebral cortex of children and young adults[1–7] and rarely the ventricles, cerebellum, brainstem, or spinal cord.[7–9] Their characteristic histopathological feature is the *astroblastic pseudorosette*.[1] These glial fibrillary acidic protein (GFAP)–immunoreactive structures consist of monopolar or less commonly cuboidal tumor cells radially oriented around a central blood vessel and thus represent a type of perivascular pseudorosette (Fig. 1). Astroblastomas are separated into low-grade or "well-differentiated" tumors, demonstrating low proliferative activity, and high-grade tumors exhibiting conspicuous mitotic activity and/or necrosis.[2,3] Low-grade ABs are often cured by gross total resection, while high-grade ABs may be associated with relatively short survival.[2–4,10,11] A few low-grade ABs have been reported to be clinically aggressive, however, and some high-grade AB patients have experienced prolonged survival with aggressive surgical and/or adjuvant therapy.[4,6,11–14] Because of this variable clinical behavior, ABs have yet to be assigned World Health Organization (WHO) tumor grades,[3] and histological parameters distinguishing clinically benign ABs from aggressive examples are not well defined. Furthermore, there appears to be a relatively high degree of discordance among neuropathologists in making the diagnosis of AB.

In this study we reviewed the clinical and histological features of a series of 28 ABs and tested for contemporary glioma biomarkers. The latter included Ki-67 protein labeling index, isocitrate dehydrogenase 1 (IDH1) R132H mutant protein expression, alpha thalassemia/mental retardation syndrome X-linked (ATRX) protein expression, SWItch/Sucrose NonFermentable-related matrix-associated actin-dependent regulator of chromatin subfamily B member 1 (SMARCB1/INI1) protein expression, O^6-methylguanine methyltransferase (MGMT) gene promoter hypermethylation, and the V600E mutation of the B-Raf serine-threonine kinase gene (*BRAF*^{V600E}). We then performed statistical analyses to test which of these parameters correlated with patient survival.

Methods

Histopathology

Studies were performed under institutional review board approved protocols. Cases diagnosed as AB at tertiary care centers were centrally reviewed by the first 2 authors. Histological criteria for inclusion in the study were as follows: (i) the presence of astroblastic pseudorosettes, occurring at least focally back to back or nearly so, and comprising at least 50% of the specimen; (ii) cuboidal, columnar, or tapered perivascular cellular processes, occasionally ending in broad endfeet; and (iii) absence of definitive features of other CNS neoplasms. Immunohistochemistry for Ki-67, ATRX, Olig2, IDH1^{R132H}, and SMARCB1/INI1 was performed using standard methods as described in the Supplementary material. Mitotic count and the Ki-67 labeling index were determined in the most actively proliferating areas of tumors.

MGMT Promoter Methylation

DNA (250 ng) extracted from formalin-fixed, paraffin-embedded tissues (Qiagen QIAamp DNA Micro Kit) was bisulfite treated (EZ DNA Methylation Kit, Zymo Research) and 3 µL was amplified in a 50 µL reaction (Qiagen HotStar DNA Polymerase Kit). Primers spanning 5 cytosine–phosphate–guanine (CpG) islands in region +17 to +39 of the *MGMT* gene, included in the CpG MGMT Kit (Qiagen), were annealed at 55°C for PCR. Pyrosequencing was performed with 30 µL of amplicon using the PyroMark Q96 ID (Qiagen). The threshold value for hypermethylation established at The Ohio State University is when the average methylation rate of 5 CpG islands is equal to or greater than 10%.

BRAF^{V600E} Mutation Analysis

Somatic mutation analyses for *BRAF*^{V600E} were performed using a single nucleotide extension assay (SNaPshot Multiplex System, Life Technologies) and results were confirmed with Sanger sequencing.

Statistics

Data were analyzed using SPSS statistical analysis software v20 (IBM). Univariate analyses were conducted using Fisher's exact test, and Pearson chi-square was used for categorical data. Student's independent sample *t*-test and the Mann–Whitney *U*-test were employed for continuous data. Survival analyses were conducted using Kaplan–Meier (KM) (Mantel–Cox log rank) and Cox proportional

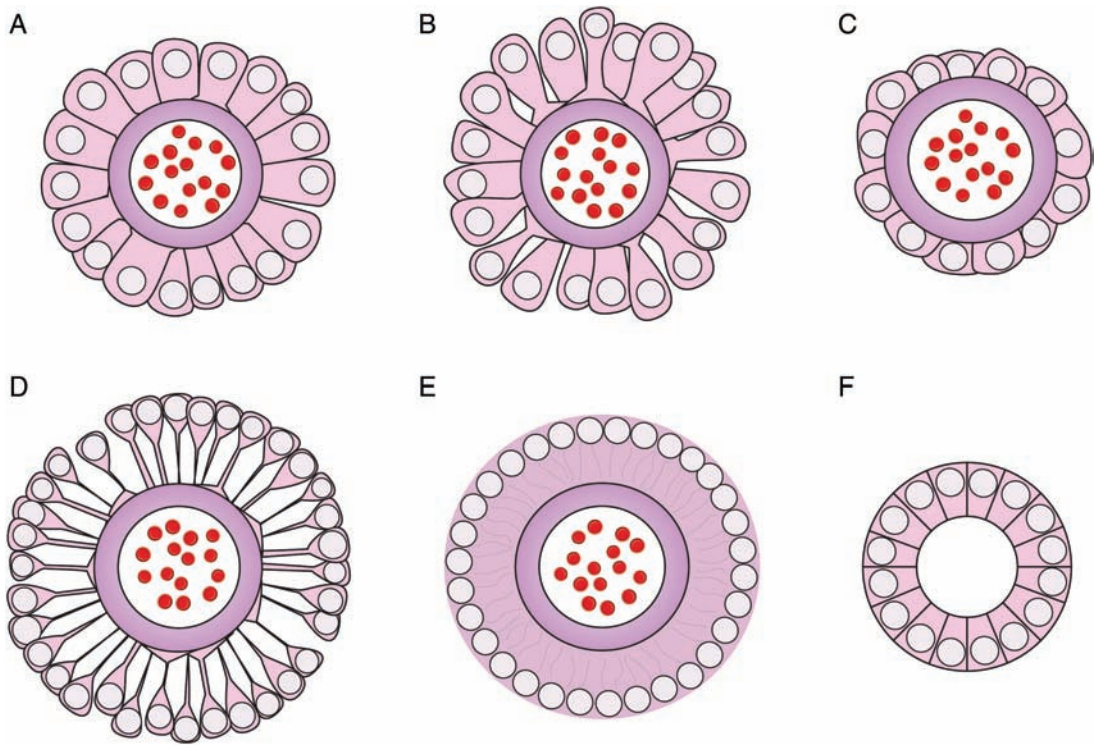

Fig. 1 Astroblastic pseudorosettes and ependymal rosettes. (A) Astroblastic pseudorosette with stout columnar-like cells occasionally demonstrating expanded endfeet. (B) Astroblastic pseudorosette displaying tapered cells. Note "bell-bottom" endfeet. (C) Astroblastic pseudorosette with cuboidal cells. Similar perivascular pseudorosettes may be seen in some ependymomas. In contrast to AB, however, ependymomas are Olig2 negative and lack other AB histological features. (D) Infrequently, astroblastomas may contain astroblastic pseudorosettes exhibiting spindly perivascular cells necessitating further distinction of such tumors from angiocentric gliomas, pilocytic/pilomyxoid astrocytomas, tanycytic ependymomas, and myxopapillary ependymomas. Even spindly cells within astroblastic pseudorosettes occasionally show flared endfeet, however, which are usually lacking in the latter tumors. In practice, individual ABs frequently demonstrate multiple astroblastic pseudorosette cell types both within a given astroblastic pseudorosette and between individual pseudorosettes. (E) Typical classic ependymal perivascular pseudorosette showing a fibrillary perivascular area lacking the more distinct cell borders seen in ABs. Note that as in astroblastic pseudorosettes, cell processes are radially oriented (depicted by the faint gray lines in the anuclear perivascular zone). (F) True ependymal rosettes lacking central blood vessels may be seen in classic ependymomas and some cortical ependymal tumors and are only rarely seen in ABs.[11] Cartoons are not drawn to scale.

hazards regression analyses. Cutoff values for continuous data (age, Ki-67 labeling index, and mitotic index) were determined using the receiver operating characteristic (ROC) method. All tests were 2-sided and a *P*-value of .05 was considered statistically significant.

Results

Patients and Histology

Twenty-seven AB cases diagnosed in university hospitals from 1992 to 2015 and 3 older archival cases from the former Armed Forces Institute of Pathology were histologically reviewed. One of the latter cases showed significant overlapping features with pilocytic astrocytoma, and one of the former was most consistent with glioblastoma. The remaining 28 cases met our inclusion criteria for AB and were further studied. Patient age at presentation ranged from 4 to 71 years (Supplementary Fig. S1). Average and median ages were 28 and 22.5 years, respectively. The observed age distribution of AB in this series thus confirms its pediatric and young adult predominance; however, patients also presented in the fifth, sixth, and eighth decades (14.3%, 10.7%, and 3.6%, respectively).

Seventeen patients were female and 11 were male, corresponding to a ratio of 1.5:1 (Supplementary Fig. S1). This was less than the previously reported ratios of 2:1 to 11:1[5,6] but similar to the 1.3:1 ratio found in a prior histopathological study of 23 cases.[4] An epidemiologic study of 239 AB cases in the Surveillance, Epidemiology, and End Results cancer registry, however, revealed an equal male-to-female ratio.[15] Nonetheless, any female predominance of AB is likely lower than previously thought. Tumor location data were available for the 26 cases diagnosed from 1992 to 2015 (Table 1). Thirteen tumors occurred in the left cerebral

Table 1 Astroblastoma biomarkers

Case No.	Age	Gender	Original Diagnosis	Revised Diagnosis Based on Mitotic Count ≥5	Location	MGMT Methylation	$BRAF^{V600E}$	Olig2	INI1	ATRX	$IDH1^{R132H}$	Mitoses/10 HPF	Ki-67%	Survival (mo)
1	10	F	AB	AB	L Parietal	–	–	+	+	+	–	0	1	143[a]
2	17	M	HGAB	AB	Cervical cord	–	NA	+	+	+	–	3	15	186[a]
3	16	F	HGAB	AB	L Parieto-occipital	–	–	+	+	+	–	3	20	100[a]
4	44	F	HGAB	AAB	L Temporal & Occipital	+	–	–	+	NA	NA	75	25	[b]
5	33	M	HGAB	AAB	L Temporal	+	+	+	+	+	–	13	15	8
6	33	F	AB	AB	R Frontal	–	+	+	+	NA	–	2	5	59
7	33	F	HGAB	AB	L Temporal	–	–	+	+	+	–	3	0	78[a]
8	40	F	AB	AB	R Medial Temporal	–	–	+	+	+	–	0	7	128[a]
9	38	F	AB	AB	R Medial Frontal	+	+	+	+	+	–	2	10	122[a]
10	12	F	AB	AB	R Fronto-parietal	–	–	+	+	+	–	0	4	106[a]
11	25	F	HGAB	AB	R Occipital	–	+	+	+	+	–	4	20	100[a]
12	12	F	HGAB	AB	R Frontal	–	+	+	+	+	–	3	17	2
13	9	F	HGAB	AAB	R Fronto-parietal	–	–	+	+	+	–	14	25	33[a]
14	71	F	HGAB	AAB	L Occipital	–	–	–	+	+	–	5	4	18
15	40	M	HGAB	AAB	R Temporal	–	NA	+	+	+	–	5	10	1
16	8	M	AB	AB	L Temporal	–	–	+	+	+	–	0	0	105[a]
17	20	F	HGAB	AB	L Occipital	–	+	+	+	+	–	3	10	238[a]
18	9	M	AB	AB	L Parasagittal	–	NA	+	+	+	–	0	3	222a
19	36	M	HGAB	AAB	R Frontal	–	–	+	+	+	–	10	45	211[a]
20	55	M	HGAB	AB	L Parietal	–	–	+	+	+	–	2	25	40
21	4	F	HGAB	AB	L Parieto-occipital	–	–	+	+	+	–	3	15	92[a]
22	9	M	HGAB	AAB	R Parietal	–	–	+	+	+	–	6	15	47
23	20	F	HGAB	AB	R Temporal	–	+	+	+	+	–	3	22	3[a]
24	20	F	AB	AB	L Parietal	–	+	+	+	+	–	2	10	38[a]
25	14	M	HGAB	NA	L Temporal	NA	NA	NA	NA	NA	NA	NA	10	39
26	58	F	HGAB	AAB	R Parietal	–	NA	+	+	+	–	5	NA	184
27	42	M	AB	AB	NA	NA	NA	NA	NA	NA	NA	0	NA	NA
28	51	M	HGAB	AAB	NA	NA	NA	NA	NA	NA	NA	8	NA	NA
				Percentage of cases positive		12	38	92	100	100	0			

AB, astroblastoma; HGAB, high-grade astroblastoma (original diagnosis); AAB, anaplastic astroblastoma (reclassified diagnosis based on mitotic count ≥5). NA, data not available due to lack of sufficient tissue or available clinical follow-up.

[a]The patient is still alive at most recent follow-up.

[b]The patient is deceased; however, the length of survival could not be ascertained.

hemisphere, 12 in the right hemisphere, and 1 in the cervical spinal cord. Ten cases involved the parietal lobe, 8 were in the temporal lobe, 5 the occipital lobe, and 5 the frontal lobe. One case was described only as left parasagittal. Of those presenting in more than one lobe, 2 were frontoparietal, 2 were parietooccipital, and 1 was temporooccipital. The parietal and temporal lobes were thus the most common regions involved by AB in this series.

Tumors originally diagnosed as high-grade ($n = 19$) were twice as common as low-grade examples ($n = 9$). A designation of "high-grade" was made based on mitotic activity ≥3/10 high-power fields (hpf) (17/19 cases; Table 1), the presence of necrosis (16/19 cases; Supplementary Table S1), and/or small primitive-appearing cells (3/19 cases). No case demonstrating zero mitoses (6/28) showed necrosis and no case exhibiting necrosis (16/28) was without detectable mitotic activity. Five cases with mitotic counts ranging from 2 to 6/10 hpf, however, lacked necrosis.

Two major histological patterns of astroblastic pseudorosettes were identified: those exhibiting columnar-like monopolar cells, varying from stout to tall, frequently with outwardly expanded broad endfeet palisading around blood vessels (Figs 1 A; 2 A, E, P, T; 3 F, K, N), and those exhibiting monopolar cells with tapered processes sometimes ending in flared "bell-bottom" endfeet (Figs 1 B; 2 D, H; Supplementary Table S1). Less prevalent patterns were cuboidal or polygonal perivascular cells, sometimes with relatively scant cytoplasm (Figs 1 C; 2 B, G; 3 G), and more rarely, perivascular cells with tapering spindly processes (Figs 1 D; 2 N, O). Nonetheless, some characteristic type A or B astroblastic pseudorosettes are usually focally present even in ABs in which type C or D astroblastic pseudorosettes predominate, which should be helpful in diagnosing AB. An additional common feature was occasional monopolar cells within astroblastic pseudorosettes demonstrating perinuclear cytoplasmic clearing exhibiting a "light bulb"-like appearance (Figs 2 E; 3 K, N).

Tumor cell nuclei were generally round and relatively uniform, often vesicular, and with a small but distinct nucleolus. In some cells the chromatin was evenly distributed and finely granular, similar to that of ependymomas. Several cases exhibited occasional vacuole-like intranuclear pseudoinclusions (Figs 2 G, H; 3 I). Rarely, large atypical nuclei resembling those seen in pleomorphic xanthoastrocytoma (PXA) were observed (Fig. 3 I).

Gemistocytic and rhabdoid cells were frequently found within cellular areas between astroblastic pseudorosettes (Supplementary Table S1). The former resembled minigemistocytes of oligodendrogliomas or were intermediate in size between minigemistocytes and classic astrocytoma gemistocytes (Figs 2 R; 3 D, J, M). Rhabdoid cells appeared similar to gemistocytic cells, except that they harbored a round pale or eosinophilic cytoplasmic inclusion (Figs 2 C, R; 3 D, E, M, P, Q). Other observed cell types included "signet-ring" or adipocyte-like cells and polygonal cells with clear or vacuolated cytoplasm, sometimes imparting a bubbly appearance to the tumor (Figs 2 A and 3 J; Supplementary Table S1). Additionally, small primitive-appearing cells with dense chromatin were present in 3 cases (Fig. 2 J, K, N, T), all of which showed increased mitotic activity (5 to 8/10 hpf). Rare large bubbly cells (Fig. 3 C and I) and oligodendroglioma-like cells (Fig. 2 H) were each also noted in 3 cases. Calcifications were occasionally present, and one case showed ossification. Notably, most of these variant features have been previously described in individual AB case reports.[2,11,14,16]

Surprisingly, eosinophilic granular bodies (EGBs) were identified in several cases (Supplementary Table S1). These were often relatively pale and finely granular (Fig. 3 B); however, some were brightly eosinophilic and coarsely granular, like classic EGBs (Fig. 2 F). Occasionally, eosinophilic granular material appeared to be extracellular (Fig. 2 R) or was present within gemistocytic cells (Figs 2 L; 3 I, J, M). Intracellular eosinophilic granular material has also been observed in granular cell astrocytomas[17,18] and oligodendrogliomas.[19,20] These structures were thought to represent tiny Rosenthal fibers in some cases[18,20] and autophagic lysosome-related structures in others.[17,19] In the latter case, their presence may suggest autophagic degeneration, possibly partially explaining the often cystic neuroimaging features of ABs.[5] Interestingly, other tumors commonly exhibiting EGBs are often cystic (ie, pilocytic astrocytomas, gangliogliomas, and PXAs).

Astroblastomas also occasionally demonstrated pale homogenous hyaline spherical bodies not obviously associated with a cellular nucleus. Many of these appeared membrane bound and may represent cross sections of cellular inclusions (Figs 2 G, H, L; 3 D, N). The nature of these hyaline bodies and extent that they may or may not represent the same process or be related to rhabdoid cell inclusions or eosinophilic granular material are unknown and require further study.

As described by Bailey and Bucy in their 1930 description of AB,[1] multinucleated cells and lymphocytic infiltrates were frequently observed (Supplementary Table S1). The latter were usually perivascular and were present in ~60% of our cases (Figs 2 P, Q; 3 A). Multinucleated tumor cells were larger than surrounding tumor cells, but not as large as typical glioma "giant cells" (Fig. 2 G, H, R) and were occasionally present within astroblastic pseudorosettes (Figs 2 E; 3 K, O).

Central vessels of astroblastic pseudorosettes showed variable degrees of hyalinization, even in high-grade tumors (Figs 2 A, D, G, O; 3 L). Some astroblastic pseudorosettes demonstrated separation of basal lamina-bound tumor cell process from the vessel wall similar to the pseudorosettes of myxopapillary ependymomas (Figs 2 O, P, Q; 3 N, O). Others contained redundant central vessels reminiscent of vascular proliferation seen in low-grade gliomas such as pilocytic astrocytoma and ganglioglioma (Figs 2 O, P, Q; 3 O).

BRAF^{V600E} Mutation Analysis

BRAF ^{V600E} mutation was found in 8 of 21 cases (38%) in which adequate DNA was available (Table 1). Seven occurred in female patients ranging from 12 to 38 years of age. The single male patient with a mutation presented at 33 years of age. *BRAF*^{V600E} mutant cases were thus clustered in a narrow age group comprising the second to early fourth decades of life (mean 25 y) (Supplementary Fig. S1). In contrast, the frequency of *BRAF*^{V600E} mutations in gangliogliomas was reported to be greatest in patients presenting in the first decade, gradually decreasing thereafter.[21] The patient age distribution of *BRAF*^{V600E} mutations observed for AB more closely resembles that of PXA.[22]

All *BRAF*^{V600E} positive AB cases showed mitotic activity, demonstrated rhabdoid cells, and showed at least a focal papillary-like structure (Table 1, Fig. 3; Supplementary Table S1). Most but not all *BRAF*^{V600E} negative tumors also

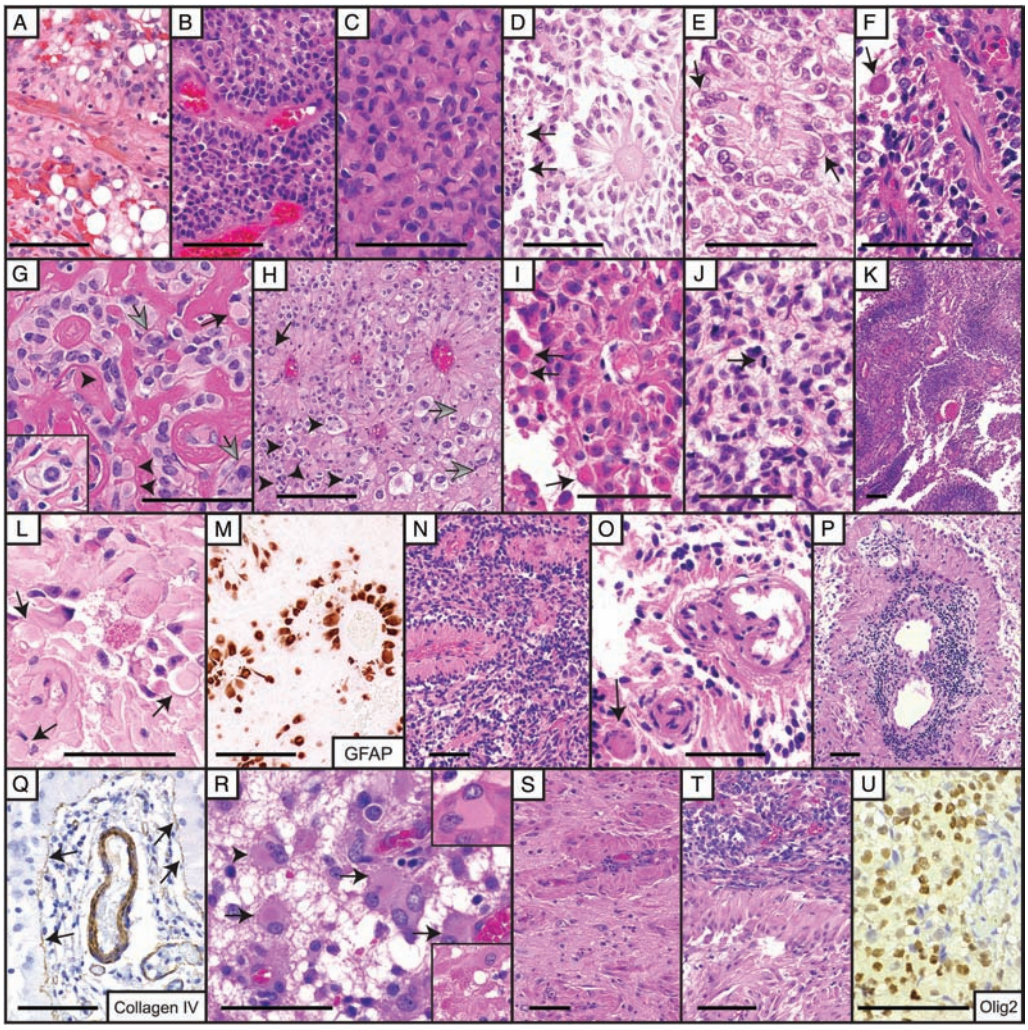

Fig. 2 Astroblastoma histological features. *Case 1:* (A) Astroblastic pseudorosette in longitudinal section. Numerous signet ring or adipocyte-like cells are present. *Case 2:* (B) Astroblastic pseudorosette cells are cuboidal to stout columnar in shape. (C) An area of rhabdoid cells is depicted. *Case 3:* (D) Astroblastic pseudorosettes. Necrosis is present on the left (arrows). Note retinoblastoma florette-like or "cartwheel" appearance of the astroblastic pseudorosettes. *Case 4:* (E) Astroblastic pseudorosette in anaplastic AB showing multinucleated "light bulb" cells (arrows). Abundant atypical mitoses and rare pleomorphic nuclei were also present (not shown). This case nevertheless demonstrated a sharp border with brain tissue. *Case 18:* (F) Astroblastic pseudorosettes in longitudinal section and EGB (arrow). *Case 10:* (G) AB showing extensive vascular sclerosis. Rhabdoid cells with pale cytoplasmic bodies (arrows) and apparent acellular pale hyaline spherical bodies (arrowheads) were noted. Multinucleated cells (gray arrow) and occasional cells with nuclear pseudoinclusions (inset, same scale as main panel) were present. Recurrent tumor lacked this extensive sclerosis. *Case 20:* (H) Large astroblastic pseudorosettes. A nuclear pseudoinclusion is indicated by the black arrow. Frequent multinucleate cells (arrowheads) and pale spherical bodies (gray arrows) were present. Large clear cells reminiscent of those seen in PXAs are also seen in the photomicrograph, as well as smaller cells with perinuclear clearing resembling oligodendrocytes. *Case 28:* (I) Anaplastic AB composed mainly of astroblastic pseudorosettes. Perivascular cells were frequently tapered and showed occasional flared endfeet. Rhabdoid cells contained brightly eosinophilic inclusions (arrows). (J) A smaller component of the tumor consisted of small undifferentiated-appearing cells demonstrating mitotic activity (arrow). (K) Pseudopalisading necrosis encompassing area of small cells. *Case 19:* (L) Brightly eosinophilic granules appeared to be both intracellular and extracellular. (M) GFAP immunohistochemical stain demonstrating stout perivascular cells in an anaplastic astroblastoma. Cells between astroblastic pseudorosettes were mostly GFAP negative. *Case 26:* (N) Anaplastic AB showing numerous small undifferentiated-appearing cells between astroblastic pseudorosettes. (O) Astroblastic pseudorosettes demonstrating retraction of perivascular cells from central vascular proliferation. Note that although very narrow, the cellular processes are of mixed columnar and tapered forms. The arrow indicates a thrombosed astroblastic pseudorosette central vessel. *Case 22:* (P) Large astroblastic pseudorosette in an anaplastic astroblastoma demonstrating retraction from a folded central vessel and smaller vessels. Tall perivascular cells with flared endfeet are separated from the vessel by a lymphocytic infiltrate. (Q) Collagen IV immunohistochemical stain demonstrating immunopositivity of basal lamina attached to retracted perivascular cells (arrows). (R) Scattered rhabdoid (arrows) and multinucleate cells (arrowhead) were present. The upper right inset depicts a gemistocytic cell. The lower right inset shows apparent extracellular eosinophilic granular material (insets same scale as main panel). (S) Tumor infiltrated brain parenchyma along blood vessels, but retained radially oriented cell rosetting. (T) Primitive-appearing small cells were focally present, here in the subarachnoid space abutting well-differentiated subpial tumor. Increased mitotic activity and occasional apoptotic cells were noted among these small cells. (U) Olig2 immunoreactivity was of variable intensity. All scale bars = 100 μm.

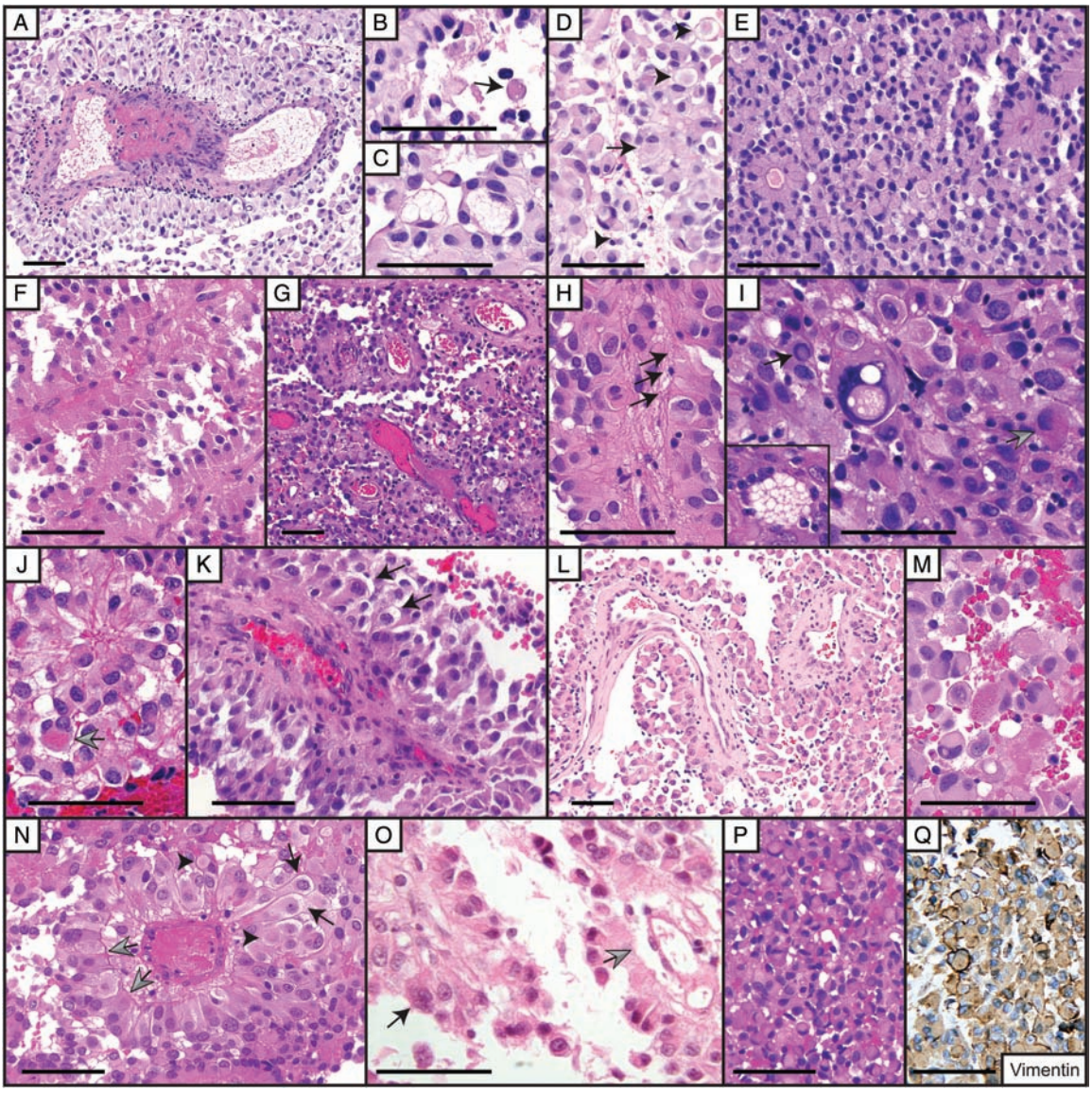

Fig. 3 Histology of $BRAF^{V600E}$ positive astroblastomas. *Case 5:* (A) Large astroblastic pseudorosette within an anaplastic astroblastoma demonstrating a small perivascular lymphocytic infiltrate and intravascular thrombosis. (B) Eosinophilic granular body near astroblastic pseudorosette (arrow). (C) Large cells with bubbly cytoplasm. (D) Astroblastic pseudorosettes associated with a rhabdoid cell (arrow) and membrane bound pale spherical bodies possibly representing transected rhabdoid cells (arrowheads). *Case 6:* (E) Astroblastic pseudorosettes and rhabdoid cells. Clear and vacuolated cells are also present. *Case 9:* (F) Astroblastoma with stout columnar perivascular cells. Occasional rhabdoid cells are present. *Case 11:* (G) Papillary-like arrangement of astroblastic pseudorosettes with mostly polygonal perivascular cells. (H) Longitudinally oriented astroblastic pseudorosette demonstrating perivascular cells with flared endfeet (arrows). (I) Rare large vacuolated tumor cell nucleus reminiscent of those seen in PXA. A cell demonstrating a single nuclear pseudoinclusion (black arrow) and a gemistocytic cell with eosinophilic granular cytoplasm (gray arrow) are also present. The inset depicts a large cell with bubbly cytoplasm and multiple peripherally located nuclei (same scale as main panel). *Case 17:* (J) Astroblastic pseudorosette with nearby gemistocytic cell containing eosinophilic granules (arrow). (K) Recurrent tumor demonstrating longitudinally oriented astroblastic pseudorosette displaying a multinucleated perivascular cell and perinuclear clearing (arrows). *Case 23:* (L) Pseudopapillary structure of anaplastic astroblastoma. (M) Rhabdoid cells and gemistocytic cell containing eosinophilic granules (center). *Case 12:* (N) Astroblastic pseudorosettes demonstrating retraction from the central vessel with cells apparently attached to the basement membrane (gray arrows). Some perivascular cells show perinuclear clearing (black arrows). Pale bodies are also present (arrowhead). *Case 24:* (O) Papillary-like astroblastic pseudorosettes. A multinucleated perivascular cell is denoted by the black arrow. Apparent astroblastic pseudorosette cell retraction from the central vessel is indicated by the gray arrow. (P) Focal areas of rhabdoid cells were present. (Q) Rhabdoid cells were vimentin immunopositive. All scale bars = 100 μm.

exhibited rhabdoid cells. Data for both *BRAF*^{V600E} status and lymphocytic infiltrates were available for 21 cases. Among these, all 8 *BRAF*^{V600E} positive ABs showed perivascular lymphocytic infiltrates, while one-half of *BRAF*^{V600E} negative cases did not (Supplementary Table S1). Similar to ganglioglioma,[21] the association of lymphocytic infiltrates with *BRAF*^{V600E} mutation in ABs was statistically significant (Fisher's exact test, $P = .018$). Interestingly, lymphocytic infiltrates are enriched in glioblastomas associated with neurofibromin 1 mutations.[23] Both *BRAF*^{V600E} and neurofibromin 1 mutations may activate mitogen-activated protein kinase signaling.[24] Hence, it is possible that trophic factors associated with gliomas with mitogen-activated protein kinase activation, such as interleukin-6,[25] may recruit lymphocytes.

MGMT Promoter Methylation

MGMT promoter hypermethylation was found in only 12% of cases tested, similar to the 18% rate reported in a series of 11 PXAs.[26] It was present in a 38-year-old woman, a 44-year-old woman, and a 33-year-old man (Table 1). Its absence in younger AB patients may be analogous to the tendency to see MGMT promoter hypermethylation only in adult cases of diffuse astrocytoma.[27] Two cases with MGMT promoter hypermethylation also harbored the *BRAF*^{V600E} mutation.

Olig2, ATRX, SMARCB1/INI1, and IDH1^{R132H} Immunohistochemistry

Twenty-three of 25 (92%) tumors tested were Olig2 positive (Table 1). Nuclear staining intensity was occasionally weak and overall more variable than in oligodendrogliomas (Fig. 2 U). No tumor showed loss of nuclear ATRX protein immunoreactivity when appropriate internal control immunoreactivity was present ($n = 23$) (Table 1). SMARCB1/INI1 protein immunostaining was intact and IDH1^{R132H} mutant protein immunostaining was negative

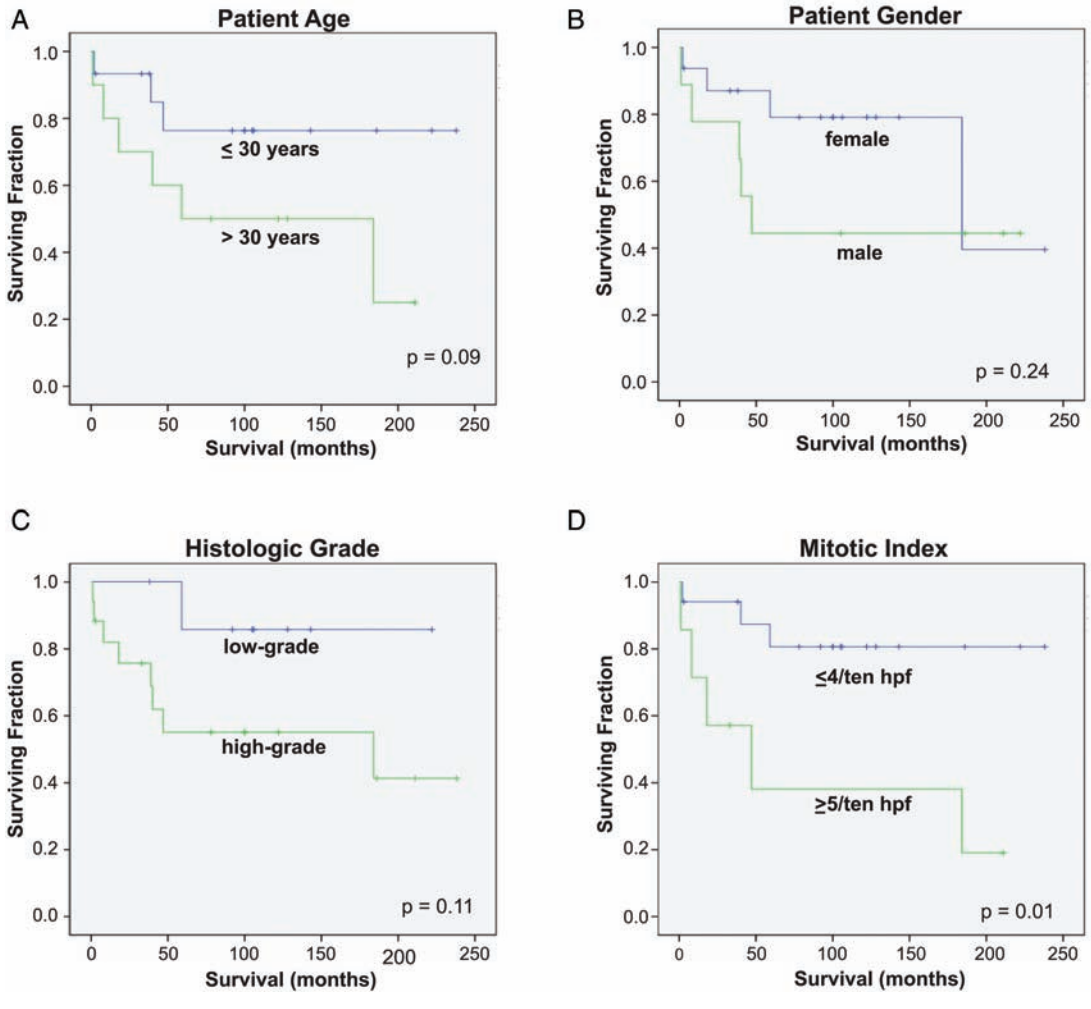

Fig. 4 Correlates of AB patient survival. Kaplan–Meier analysis curves are shown for (A) patient age, (B) patient gender, (C) histological grade, and (D) mitotic index. Although all plots appear to depict clear trends, only mitotic index showed a statistically significant relationship to patient survival using the Mantel–Cox log rank test.

Table 2 Results of statistical analyses of candidate prognostic features

Kaplan-Meier statistics (Mantel-Cox log rank)				
Variable	χ^2	*df*	*P*	*n*
Age >30 y	2.818	1	.093	24
Male gender	1.410	1	.235	24
High grade	2.597	1	.107	24
Mitoses ≥5	6.292	1	.012	24
Necrosis	0.776	1	.378	24
$BRAF^{V600E}$	0.835	1	.361	20
Ki-67 >4%	1.164	1	.281	24

Cox proportional hazards regression analysis					
Variable	Hazard Ratio	*df*	*P*	95% CI	
Age >30 y	3.086	1	.111	0.772	12.346
Male gender	2.202	1	.246	0.580	8.357
Necrosis	1.852	1	.386	0.460	7.458
$BRAF^{V600E}$	2.081	1	.371	0.418	10.368
High grade	4.752	1	.143	0.589	38.334
Ki-67 >4%	3.002	1	.305	0.368	24.469
Mitoses ≥5	5.401	1	.024	1.253	23.285
Mitoses ≥5 controlling for necrosis[a]	5.902	1	.031	1.182	29.474
Mitoses ≥5 controlling for $BRAF^{V600E}$[a]	9.424	1	.031	1.229	72.252

Indicated mitotic counts are from 10 high-power fields. χ^2 = chi square, *df* = degrees of freedom.
Sample numbers (*n*) for each variable are the same as for the KM analyses above, *df* = degrees of freedom.
[a]Hierarchical regression.

in all cases tested (*n* = 25). A recent independent study also reported no IDH1 mutations in AB.[28]

Survival Analysis

Follow-up survival data were available for 25 cases (Table 1). Mean and median follow-up were equal at 7.7 years (92 mo). Sixteen AB patients were alive at the time of last follow-up and 9 had died. Patients 30 years of age or less and female patients tended to survive longer than older or male patients (Fig. 4 A and B, Table 2). Eighty-two percent of female AB patients for whom survival information was available for at least 5 years from diagnosis (9/11 cases) were alive at 5 years, while only 44% of male patients (4/9 cases) were alive at 5 years. The overall Cox hazard ratio for male gender was 2.2; however, this did not reach statistical significance (*P* = .25), nor did it in KM analysis (*P* = .24; Table 2 A, Fig. 4 B).

Patients originally diagnosed with histologically high-grade AB also tended to show decreased survival compared with low-grade AB, but this was not statistically significant by KM analysis (*P* = .11; Table 2 A, Fig. 4 C). Cox analysis revealed an approximately 4.8-fold risk of death in high-grade AB patients; however, this was also not significant (Table 2 B).

Next we tested for a possible association of Ki-67 labeling index with survival. A Ki-67 labeling index of 4% was determined to be the best cutoff using the ROC method. Although the KM plot suggests better survival of patients with Ki-67 labeling indices of 4% or less, this was not statistically significant (Table 2; Supplementary Fig. S2A). The presence of necrosis or the $BRAF^{V600E}$ mutation were both associated with an approximately 2-fold increased risk of death, but again neither was statistically significant (Table 2; Supplementary Fig. S2B, C).

Mitotic index data were available for 27 cases (Table 1). Mean and median mitotic counts were 6.4/10 hpf and 3/10 hpf, respectively. The ROC method yielded a cutoff value of 4 mitoses/10 hpf. Five-year survival data were available for 15 of the 18 patients showing 4 or fewer mitoses per 10 hpf, of whom 3 had died, correlating with a 5-year overall survival rate of 80.0%. Seven of 9 patients demonstrating 5 or more mitoses/10 hpf had available 5-year survival data, of whom 5 had died. The 5-year overall survival for this group was only 28.6%. These differences were statistically significant by both KM analysis (*P* = .012; Fig. 4 D) and Cox proportional hazards analysis, where 5 or more mitoses/10 hpf was associated with a 5.4-fold increased risk of patient death (*P* = .024; Table 2). After adjusting for $BRAF^{V600E}$ mutation, patients with a mitotic count of 5 or more were 9.4 times more likely to have died (*P* = .031; Table 2 B).

Discussion

Histologically, AB is most often confused with ependymoma.[2,3,11,29] Olig2 positivity, found in the majority of AB cases tested, however, appears to exclude most ependymomas.[30] Additionally, many ependymomas demonstrate true ependymal rosettes, which are generally not

conspicuous in ABs (Fig. 1 F).[11] Common histological features of AB described herein, which are usually absent in ependymoma, include frequent multinucleated cells, perivascular cells with nuclear clearing, eosinophilic granular material, lymphocytic infiltrates, rhabdoid cells, hyaline spherical bodies, and nuclear pseudoinclusions. These features are also usually absent in most diffuse gliomas, excluding glioblastoma, albeit some occur in pilocytic astrocytomas, gangliogliomas, and PXAs. The latter tumors, however, lack extensive astroblastic pseudorosettes and may show other features not found in AB, such as classic Rosenthal fibers, ganglion cells, bipolar spindle cells, or marked pleomorphism.

Unlike other AB cases, case 22 infiltrated the perivascular spaces of surrounding brain and showed subpial aggregation, mimicking angiocentric glioma (AG). Common histological features of AB described above, however, are absent in AG. Unlike ABs, AGs by definition contain bipolar cells with elongated nuclei and usually lack detectable mitotic activity.[33,34] Furthermore, in addition to radially oriented monopolar perivascular cells as seen in ABs and ependymomas, AGs also show circumferentially and longitudinally oriented perivascular growth patterns, which are absent in AB. Finally, AGs have been reported to be Olig2 negative[31,32] and lack *BRAF*^{V600E} mutations or the vascular hyalinization commonly seen in AB.[33–35] Rare reported cases of AG with astroblastoma-like features and/or increased mitotic activity[34,36] should thus be reexamined, immunostained for Olig2, and tested for BRAF mutations.

Three AB cases exhibited cells resembling oligodendrocytes. The absence of 1p/19q loss of heterozygosity or IDH1/2 mutations rules out oligodendroglioma. The latter also excludes some diffuse astrocytomas and secondary glioblastomas,[37] while ATRX positivity eliminates a subset of astrocytomas and rare ATRX-negative glioblastomas.[38] SMARCB1/INI1 immunopositivity, on the other hand, rules out most atypical teratoid/rhabdoid tumors and cribriform neuroepithelial tumors.[39]

Although this is the largest reported histopathological study of AB, statistical analyses related to survival are limited by the still relatively small number of cases and variable patient follow-up intervals resulting in censoring of some data. Furthermore, information regarding extent of surgical resection, tumor recurrence, and adjuvant therapies was not available for several cases and was not considered (available data are presented in Supplementary Table S2).

Nevertheless, some interesting patterns emerged. Patients younger than 30 years of age and females clearly appeared to live longer. Age is a known prognostic indicator for many brain neoplasms, and although variable for different tumor types, older patients generally do worse.[40] Better survival in female patients has been reported in CNS tumors overall,[41] and specifically in ependymoma, medulloblastoma, and glioblastoma.[40–42]

Of all factors examined related to AB patient survival, only mitotic count was statistically significant, strongly implicating it as the most important histological correlate of tumor behavior. Among cases for which at least 5-year follow-up data were available, 80% of patients with a mitotic count of ≤4/10 hpf were alive at 5 years compared with 28.6% of patients with mitotic counts of 5/10 hpf or greater (Table 1). Comparable 5-year survival rates reported for ependymomas are 73% for grade II tumors and 49% for grade III tumors.[41] The above overall 5-year survival rates for AB fit closely with WHO estimates that patients with grade II CNS tumors usually survive over 5 years and most with grade III tumors survive 2–3 years.[43] We therefore propose a mitotic count of 5/10 hpf or more as the critical criterion for identifying more aggressive higher-grade lesions, namely anaplastic astroblastomas. Application of this criterion resulted in the reclassification of 9 tumors originally diagnosed as high-grade AB to low-grade AB and changed the ratio of high-grade to low-grade tumors in this series from originally 2:1 to close to 1:1 (Table 1). Thus, a possible overemphasis of mitotic counts of <5/hpf and/or the presence of necrosis and resultant overgrading of tumors may account for some reported cases of "high-grade" AB associated with prolonged survival. Additional studies encompassing larger series of AB patients, including data on treatment and recurrences accompanied by expanded molecular profiles, are likely required to identify predictors of clinical behavior that would permit further histopathological or molecular stratification of ABs.

The histogenesis of AB has been an ongoing debate. Authors have argued whether ABs are more biologically related to ependymomas or diffuse astrocytomas.[2,11] Histological and molecular findings in this series suggest the answer is "neither." *BRAF*^{V600E} mutations have been reported in up to 66% of PXAs, 58% of gangliogliomas, 51% of dysembryoplastic neuroepithelial tumors, 43% of subependymal giant cell astrocytomas (SEGAs), and 33% of diencephalic and 13% of cerebral pilocytic astrocytomas.[21,22,44] They are present much less frequently in pediatric glioblastomas,[45] desmoplastic infantile astrocytomas/gangliogliomas,[46] and adult astrocytomas[22,45] and are absent in ependymomas.[22]

Albeit nonspecific, EGBs and lymphocytic infiltrates are also common in gangliogliomas, PXAs, and pilocytic astrocytomas. Nuclear pseudoinclusions and multinucleated cells are common in PXA but are also nonspecific and occur in a wide range of glial tumors. Nevertheless, combined with the similar age distribution at clinical presentation and roughly similar frequency of *BRAF*^{V600E} mutation and *MGMT* promoter hypermethylation, our findings suggest that AB and PXA may share a closely related histogenesis.

On a larger scale, all pediatric gliomas with *BRAF*^{V600E} mutations may be ontologically related, as, with the exception of SEGA and diencephalic pilocytic astrocytoma, nearly all tend to manifest as superficial cortical lesions. Pertinently, SEGA and diencephalic pilocytic astrocytoma also involve gray matter. Indeed, some of these tumors have been hypothesized to belong to a group of developmentally related gliomas with variable glial and neuronal differentiation.[47] This is not to say that ABs and ependymomas are unrelated. Their shared tendency to form perivascular pseudorosettes and demonstrate epithelial-like histomorphological characteristics clearly suggests the contrary. It is possible that ABs arise from a common radial glia-derived precursor cell representing a branch point prior to definitive ependymal or glioneuronal differentiation.[11,29,48] Regardless, AB will likely remain a controversial diagnosis prior to its definitive molecular characterization,

and should be carefully differentiated from ependymoma, and other possible *BRAF*^{V600E} mutant lesions.

Although not statistically significant, we observed a trend for ABs with *BRAF*^{V600E} to be associated with shorter patient survival (Supplementary Fig. S2C), consistent with that found for melanoma, colorectal carcinoma and papillary thyroid carcinoma.[49,50] Interestingly, a recent study of PXAs with long-term follow-up found significantly better survival for tumors with the *BRAF*^{V600E} mutation, when both low-grade and anaplastic PXAs were considered together.[51] Compounding these findings, however, was a higher frequency of *BRAF*^{V600E} in low-grade PXAs. In contrast, *BRAF*^{V600E} mutation was evenly distributed in low-grade and anaplastic ABs (based on mitotic index ≥5/10 hpf). Nevertheless, in select AB patients with *BRAF*^{V600E} and only partially resectable or recurrent tumor, BRAF inhibitor therapy may represent a potential treatment option.[52] Similarly the presence of *MGMT* promoter hypermethylation may suggest rational use of alkylating agents, such as temozolomide. We therefore recommend *BRAF* mutational analysis and *MGMT* promoter methylation testing in all suspected AB cases.

Supplementary Material

Supplementary material is available online at *Neuro-Oncology* (http://neuro-oncology.oxfordjournals.org/).

Funding

This work was supported in part by NIH grants K08 NS45077 and R01 NS081125 (to N.L.L.). Roger E McLendon is supported in part by the Pediatric Brain Tumor Foundation.

Acknowledgments

We thank Andreas von Deimling for IDH1^{R132H} immunostaining of pilot cases, Michael Kruger and Daniel Schultz for assistance with statistical analysis, and Fredrik Skarstedt for graphics assistance.

Conflict of interest statement. None declared.

References

1. Bailey P, Bucy PC. Astroblastomas of the brain. *Acta Psychiatr Neurol.* 1930;5:439–461.
2. Brat DJ, Hirose Y, Cohen KJ et al. Astroblastoma: clinicopathologic features and chromosomal abnormalities defined by comparative genomic hybridization. *Brain Pathol.* 2000;10(3):342–352.
3. Aldape KD, Rosenblum MK. Astroblastoma. In: Louis DN, Ohgaki H, Wiestler OD, Cavenee WK, eds. *WHO Classification of Tumours of the Central Nervous System*. Lyon: International Agency for Research on Cancer; 2007:88–89.
4. Bonnin JM, Rubinstein LJ. Astroblastomas: a pathological study of 23 tumors, with a postoperative follow-up in 13 patients. *Neurosurgery.* 1989;25(1):6–13.
5. Bell JW, Osborn AG, Salzman KL et al. Neuroradiologic characteristics of astroblastoma. *Neuroradiology.* 2007;49(3):203–209.
6. Salvati M, D'Elia A, Brogna C et al. Cerebral astroblastoma: analysis of six cases and critical review of treatment options. *J Neurooncol.* 2009;93(3):369–378.
7. Sughrue ME, Choi J, Rutkowski MJ et al. Clinical features and post-surgical outcome of patients with astroblastoma. *Clin Neurosci.* 2011;18(6):750–754.
8. Sabharwal P, Sadashiva N, Unchagi A et al. Intraventricular astroblastoma in an infant: a case report and review of the literature. *Pediatr Neurosurg.* 2015;506:325–329.
9. Notarianni C, Akin M, Fowler M et al. Brainstem astroblastoma: a case report and review of the literature. *Surg Neurol.* 2008;69(2):201–205.
10. Thiessen B, Finlay J, Kulkarni R et al. Astroblastoma: does histology predict biologic behavior? *J Neurooncol.* 1998;40(1):59–65.
11. Lehman NL. Central nervous system tumors with ependymal features: a broadened spectrum of primarily ependymal differentiation? *J Neuropathol Exp Neurol.* 2008;67(3):177–188.
12. Kaji M, Takeshima H, Nakazato Y et al. Low-grade astroblastoma recurring with extensive invasion. *Neurol Med Chir (Tokyo).* 2006;46(9):450–454.
13. Miranda P, Lobato RD, Cabello A et al. Complete surgical resection of high-grade astroblastoma with long time survival: case report and review of the literature. *Neurocirugia (Astur).* 2006;17(1):60–63.
14. Nasit JG, Trivedi P. Recurrent low-grade astroblastoma with signet ring-like cells and high proliferative index. *Fetal Pediatr Pathol.* 2013;32(4):284–292.
15. Ahmed KA, Allen PK, Mahajan A et al. Astroblastomas: a Surveillance, Epidemiology, and End Results (SEER)-based patterns of care analysis. *World Neurosurg.* 2014;82(1–2):e291–e297.
16. Yuzawa S, Nishihara H, Tanino M et al. A case of cerebral astroblastoma with rhabdoid features: a cytological, histological, and immunohistochemical study. *Brain Tumor Pathol.* 2016;33(1):63–70.
17. Brat DJ, Scheithauer BW, Medina-Flores R et al. Infiltrative astrocytomas with granular cell features (granular cell astrocytomas): a study of histopathologic features, grading, and outcome. *Am J Surg Pathol.* 2002;26(6):750–757.
18. Kinjo S, Yokoo H, Hirato J et al. Anaplastic astrocytoma with eosinophilic granular cells. *Neuropathology.* 2007;27(5):457–462.
19. Takei Y, Mirra SS, Miles ML. Eosinophilic granular cells in oligodendrogliomas. An ultrastructural study. *Cancer.* 1976;38(5):1968–1976.
20. Yoshida T, Nakazato Y. Characterization of refractile eosinophilic granular cells in oligodendroglial tumors. *Acta Neuropathol.* 2001;102(1):11–19.
21. Koelsche C, Wöhrer A, Jeibmann A et al. Mutant BRAF V600E protein in ganglioglioma is predominantly expressed by neuronal tumor cells. *Acta Neuropathol.* 2013;125(6):891–900.
22. Schindler G, Capper D, Meyer J et al. Analysis of BRAF V600E mutation in 1,320 nervous system tumors reveals high mutation frequencies in pleomorphic xanthoastrocytoma, ganglioglioma and extra-cerebellar pilocytic astrocytoma. *Acta Neuropathol.* 2011;121(3):397–405.
23. Rutledge WC, Kong J, Gao J et al. Tumor-infiltrating lymphocytes in glioblastoma are associated with specific genomic alterations and related to transcriptional class. *Clin Cancer Res.* 2013;19(18):4951–4960.
24. Brennan CW, Verhaak RG, McKenna A et al. The somatic genomic landscape of glioblastoma. *Cell.* 2013;155(2):462–477.

25. Gurgis FM, Yeung YT, Tang MX et al. The p38-MK2-HuR pathway potentiates EGFRvIII-IL-1β-driven IL-6 secretion in glioblastoma cells. *Oncogene*. 2015;34(22):2934–2942.
26. Marucci G, Morandi L. Assessment of MGMT promoter methylation status in pleomorphic xanthoastrocytoma. *J Neurooncol*. 2011;105(2):397–400.
27. Jones DT, Mulholland SA, Pearson DM et al. Adult grade II diffuse astrocytomas are genetically distinct from and more aggressive than their paediatric counterparts. *Acta Neuropathol*. 2011;121(6):753–761.
28. Asha U, Mahadevan A, Sathiyabama D et al. Lack of IDH1 mutation in astroblastomas suggests putative origin from ependymoglial cells? *Neuropathology*. 2015;35(4):303–311.
29. Kubota T, Sato K, Arishima H et al. Astroblastoma: immunohistochemical and ultrastructural study of distinctive epithelial and probable tanycytic differentiation. *Neuropathology*. 2006;26(1):72–81.
30. Švajdler M, Rychlý B, Mezencev R et al. SOX10 and Olig2 as negative markers for the diagnosis of ependymomas: An immunohistochemical study of 98 glial tumors. *Histol Histopathol*. 2016;31(1):95–102.
31. Miyata H, Ryufuku M, Kubota Y et al. Adult-onset angiocentric glioma of epithelioid cell-predominant type of the mesial temporal lobe suggestive of a rare but distinct clinicopathological subset within a spectrum of angiocentric cortical ependymal tumors. *Neuropathology*. 2012;32(5):479–491.
32. Japp A, Gielen GH, Becker AJ. Recent aspects of classification and epidemiology of epilepsy-associated tumors. *Epilepsia*. 2013;54(Suppl 9):5–11.
33. Lellouch-Tubiana A, Boddaert N, Bourgeois M et al. Angiocentric neuroepithelial tumor (ANET): a new epilepsy-related clinicopathological entity with distinctive MRI. *Brain Pathol*. 2005;15(4):281–286.
34. Wang M, Tihan T, Rojiani AM et al. Monomorphous angiocentric glioma: a distinctive epileptogenic neoplasm with features of infiltrating astrocytoma and ependymoma. *J Neuropathol Exp Neurol*. 2005;64(10):875–881.
35. Qaddoumi I, Orisme W, Wen J et al. Genetic alterations in uncommon low-grade neuroepithelial tumors: BRAF, FGFR1, and MYB mutations occur at high frequency and align with morphology. *Acta Neuropathol*. 2016;1316:833–845.
36. Ni HC, Chen SY, Chen L et al. Angiocentric glioma: a report of nine new cases, including four with atypical histological features. *Neuropathol Appl Neurobiol*. 2015;41(3):333–346.
37. Nobusawa S, Watanabe T, Kleihues P et al. IDH1 mutations as molecular signature and predictive factor of secondary glioblastomas. *Clin Cancer Res*. 2009;15(19):6002–6007.
38. Wiestler B, Capper D, Holland Letz T et al. ATRX loss refines the classification of anaplastic gliomas and identifies a subgroup of IDH mutant astrocytic tumors with better prognosis. *Acta Neuropathol*. 2013;126(3):443–451.
39. Ibrahim GM, Huang A, Halliday W et al. Cribriform neuroepithelial tumour: novel clinicopathological, ultrastructural and cytogenetic findings. *Acta Neuropathol*. 2011;122(4):511–514.
40. Ostrom QT, Gittleman H, Fulop J et al. CBTRUS statistical report: primary brain and central nervous system tumors diagnosed in the United States in 2008-2012. *Neuro Oncol*. 2015;17(Suppl 4):iv1–iv62.
41. Rodríguez D, Cheung MC, Housri N et al. Outcomes of malignant CNS ependymomas: an examination of 2408 cases through the Surveillance, Epidemiology, and End Results (SEER) database (1973-2005). *J Surg Res*. 2009;156(2):340–351.
42. Perry A. Medulloblastomas with favorable versus unfavorable histology: how many small blue cell tumor types are there in the brain? *Adv Anat Pathol*. 2002;9(6):345–350.
43. Kleihues P, Louis DN, Wiestler OD et al. WHO grading of tumours of the central nervous system. In: Louis DN, Ohgaki H, Wiestler OD, Cavenee WK, eds. *WHO Classification of Tumours of the Central Nervous System*. Lyon: International Agency for Research on Cancer; 2007:10–11.
44. Lee D, Cho YH, Kang SY et al. BRAF V600E mutations are frequent in dysembryoplastic neuroepithelial tumors and subependymal giant cell astrocytomas. *J Surg Oncol*. 2015;111(3):359–364.
45. Dahiya S, Emnett RJ, Haydon DH et al. BRAF-V600E mutation in pediatric and adult glioblastoma. *Neuro Oncol*. 2014;16(2):318–319.
46. Koelsche C, Sahm F, Paulus W et al. BRAF V600E expression and distribution in desmoplastic infantile astrocytoma/ganglioglioma. *Neuropathol Appl Neurobiol*. 2014;40(3):337–344.
47. Powell SZ, Yachnis AT, Rorke LB et al. Divergent differentiation in pleomorphic xanthoastrocytoma. Evidence for a neuronal element and possible relationship to ganglion cell tumors. *Am J Surg Pathol*. 1996;20(1):80–85.
48. Rubinstein LJ, Herman MM. The astroblastoma and its possible cytogenic relationship to the tanycyte. An electron microscopic, immunohistochemical, tissue- and organ-culture study. *Acta Neuropathol*. 1989;78(5):472–483.
49. Safaee Ardekani G, Jafarnejad SM, Tan L et al. The prognostic value of BRAF mutation in colorectal cancer and melanoma: a systematic review and meta-analysis. *PLoS One*. 2012;7(10):e47054.
50. Xing M, Alzahrani AS, Carson KA et al. Association between BRAF V600E mutation and mortality in patients with papillary thyroid cancer. *JAMA*. 2013;309(14):1493–1501.
51. Ida CM, Rodriguez FJ, Burger PC et al. Pleomorphic xanthoastrocytoma: natural history and long-term follow-up. *Brain Pathol*. 2015;25(5):575–586.
52. Usubalieva A, Pierson CR, Kavran CA et al. Primary meningeal pleomorphic xanthoastrocytoma with anaplastic features: a report of two cases, one with BRAF V600E mutation and clinical response to the BRAF inhibitor dabrafenib. *J Neuropathol Exp Neurol*. 2015;74(10):960–969.